Annals of Nuclear Medicine Vol. 12, No. 6, 333–339, 1998

A comparison of Tc-99m HMPAO brain SPECT images of young and aged normal individuals

Ryoi GOTO, Ryuta KAWASHIMA, Hiroshi ITO, Masamichi KOYAMA, Kazunori SATO, Shuichi ONO, Seiro YOSHIOKA and Hiroshi FUKUDA

Department of Nuclear Medicine and Radiology, Division of Brain Sciences, Institute of Development, Aging and Cancer (IDAC), Tohoku University

The purpose of this study was to examine the normal distribution patterns of ^{99m}Tc-HMPAO (HMPAO) in young and aged normal individuals and to clarify differences between the distribution patterns of the two groups by means of an anatomical standardization technique.

The tracer distribution was measured with HMPAO and SPECT in 18 normal subjects; age range 20–81 yrs. SPECT images were globally normalized by averaging whole brain radioactivity counts to 100 counts/voxel. The SPECT images for each subject were transformed into the standard brain anatomy by means of a computerized brain atlas, together with each subject's CT images. Mean and SD images for young (28.8 ± 6.4 yrs) and aged groups (62.3 ± 10.2 yrs) were then calculated on a voxel-by-voxel basis.

Statistically significant differences between young and aged groups were observed in the relative tracer distribution patterns. In the aged group, relative decreases were found in the cortical areas of the frontal and temporal lobes, limbic areas and basal ganglia regions.

The results, as visualized changes in tracer distribution patterns with aging, may contribute to more accurate clinical diagnosis.

Key words: SPECT, aging, anatomical standardization

INTRODUCTION

TECHNETIUM-99m HMPAO [hexamethyl propylene amine oxime] (HMPAO) is widely used with single photon emission tomography (SPECT).[1] This lipid soluble agent rapidly passes through the intact blood brain barrier and stays fixed within the brain tissue.[2] Despite the wide use of HMPAO, however, the normal distribution pattern and age-related changes in SPECT images have yet to be comprehensively detailed.

An anatomical standardization technique, which has been commonly used in recent positron emission tomography (PET) studies, enables group comparison on a voxel-by-voxel basis by transforming individual brain images into the standard shape in the stereotaxic space.[3–5] In order to clarify the normal distribution patterns of HMPAO-SPECT and to estimate the differences between normal young and aged individuals, we applied this anatomical standardization technique with the computerized brain atlas of Roland et al.[3]

Received May 19, 1998, revision accepted September 16, 1998.

For reprint contact: Ryoi Goto, M.D., Department of Nuclear Medicine and Radiology, Division of Brain Sciences, Institute of Development, Aging and Cancer (IDAC), Tohoku University, 4–1 Seiryo-machi, Aoba-ku, Sendai 980–8575, JAPAN.

MATERIALS AND METHODS

Subjects

Ten young (all males; age: 28.8 ± 6.4) and eight aged volunteers (3 males, 5 females; age: 62.3 ± 10.2) participated in this study (Table 1). A CT scan was performed on each subject immediately after the SPECT measurement. None had any prior or present history of medical or psychiatric illness that could affect cerebral blood flow (CBF) and all had normal CT and SPECT scans judged by a neuroradiologist. All subjects were right-handed according to the H-N Handedness Inventory.[6] Written

informed consent was obtained from each volunteer on forms approved by the IDAC, Tohoku University.

In order to minimize alignment differences between the CT and SPECT, line markers representing the cantho-meatal (CM) line were drawn directly on each subject's face along the 3D laser alignment beams of the CT or SPECT apparatuses.

A brain atrophy index (BAI) was calculated from CT sections 50, 60, 70, 80 and 90 mm above the CM line with following equation, BAI = CSF/CC × 100%, where CSF and CC represent the volumes of the cerebrospinal fluid space and the cranial cavity, respectively.[7] Brain tissue, cranial bone and CSF on CT images were specified with their CT numbers. The cut-off level of the CT number for the brain from CSF was 24 and that for bone from CSF was 200.

SPECT imaging

SPECT imaging was carried out with a four-head rotating gamma camera system (HITACHI Medico SPECT 2000H). The collimators were of the low energy and high resolution (LEHR) type, providing 8 mm spatial resolution (FWHM). 1009.1 ± 57.7 MBq of ^{99m}Tc-HMPAO was used. Brain SPECT imaging started within 10 minutes after a bolus injection of the tracer into each subject through the cubital vein of the left arm. All subjects remained supine with their eyes closed from the time of the injection until completion of the measurements. SPECT data were processed with a Butterworth filter (with a dimension of 12 and a cut-off of 0.25 cycles/pixel).[8] Attenuation correction after the image reconstruction was performed by a post correction method (Chang's method).[9,10] Reconstructed images of transverse sections parallel to the CM line with a slice thickness of 8 mm through the brain were subjected to further analyses. Correction for scattered photons was not performed. Brain area was defined from the SPECT image by setting threshold at 30% of the maximun pixel value.

Anatomical standardization of SPECT images

The SPECT images were globally normalized by averaging whole brain radioactivity counts to 100 counts/pixel (image normalization). Thereupon the SPECT image of each subject was transformed into the standard brain anatomy with a computerized brain atlas.[3] We refer to this process as "image standardization," and it includes the following steps.

1. The anatomical structures of the computerized standard brain atlas, i.e., contours of the brain, main sulci and ventricles are fitted interactively to each subject's CT images with both linear and non-linear parameters in a three-dimensional space. The same parameters are subsequently used to transform each subject's CT images into the standard anatomical form. In the present study the means of anatomically standardized CT images were calculated on a voxel-by-voxel basis for each age group to estimate the accuracy of the anatomical standardization procedure.

2. Each SPECT image is then transformed into the standard brain format with the same parameters. The process minimizes morphological differences among individual brains and all subjects' SPECT images are represented as common standardized shapes in a three dimensional space.

Table 1 Subjects' ages and BAIs

group			
aged		young	
age/sex	BAI	age/sex	BAI
49/M	5.4	20/M	2.4
54/F	2.7	20/M	5.2
57/F	2.3	24/M	2.0
61/M	4.8	26/M	2.0
61/F	3.3	27/M	2.7
63/F	4.9	29/M	3.5
72/F	4.9	34/M	2.6
81/F	6.0	36/M	4.9
		36/M	5.4
		36/M	5.4

The subjects' ages and Brain Atrophy Index (BAI, see text) are shown above.

Statistics

The processed SPECT images were segregated into aged and young groups (Table 1) and the mean and SD images were calculated on a voxel-by-voxel basis. The young from the aged group subtraction SPECT images of were made on a voxel by voxel basis and vice versa. From these images descriptive three dimensional t-value images of young minus aged and aged minus young were calculated. Voxels having a t-value of over 2.6 (corresponding to a significance level of $p < 0.01$) were chosen to represent statistically significant differences between two groups.

Evaluation of age-related changes

ROIs were defined for these specific areas which showed significant differences in voxel by voxel analysis and applied to each subject's transformed SPECT image to estimate individual values. The purpose of this ROI analysis was to evaluate age-related changes in the tracer distribution pattern.

RESULTS

The representative distribution images obtained for the two age groups are shown in Figure 1. The mean images of normalized and standardized young normal subjects are shown in the top column, A. The mean images of the aged subjects are shown in the bottom column, C. The corresponding standard brain sections are shown in the middle column, B. Relative higher tracer uptake was

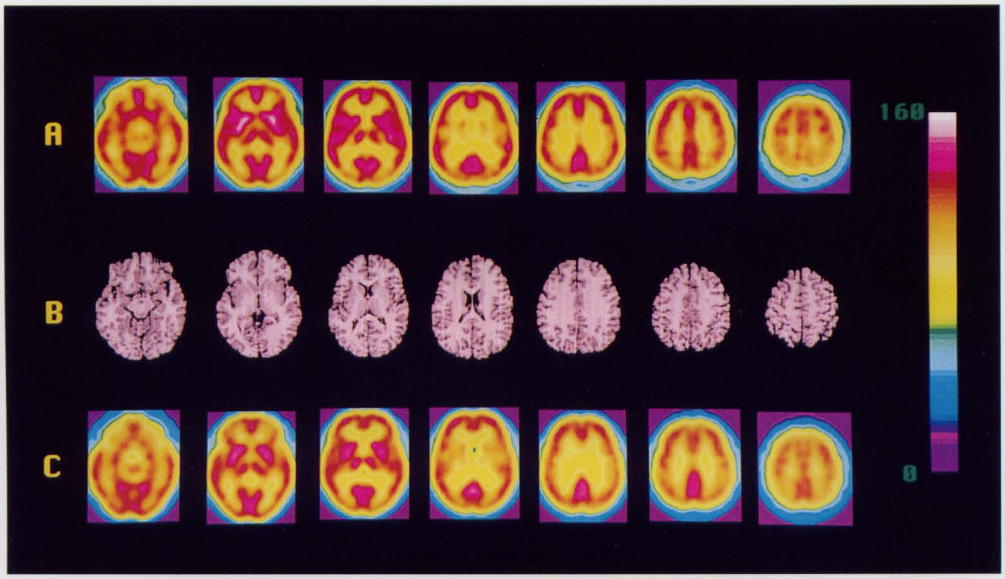

Fig. 1 The mean SPECT images of young and aged groups. The top column (A) and bottom column (C) respectively show mean HMPAO SPECT images for the 10 young and the 8 aged subjects. The middle column (B) shows the corresponding standard brain sections. The left of the image is the right hemisphere of the brain. Sections are −10, 0, 10, 20, 30, 40, 50 mm above the AC-PC line. Scale maximum and minimum values are 160 and 0 counts per pixel, respectively.

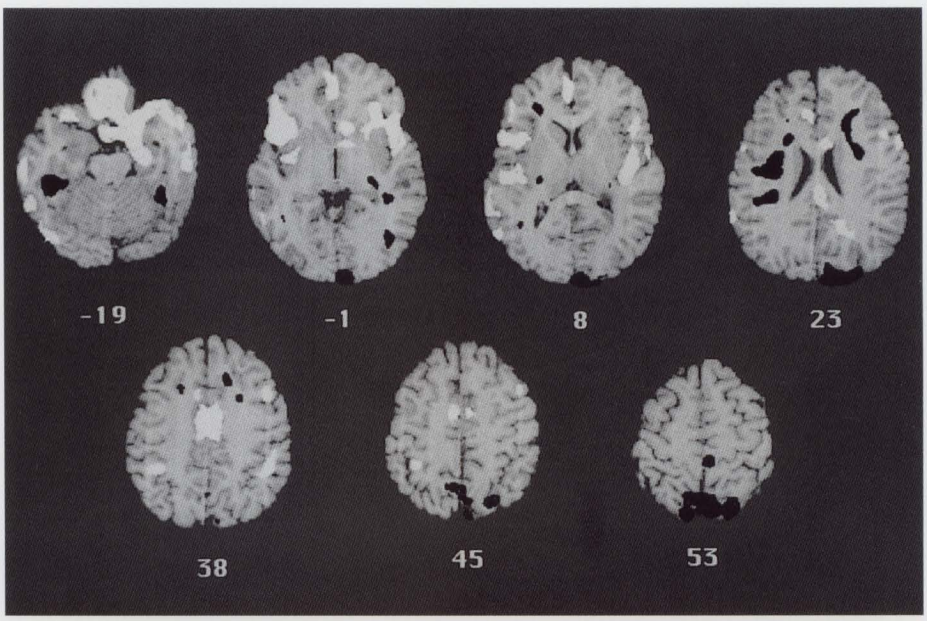

Fig. 2 Regions of significant differences superimposed on the standard brain. White and Black areas respectively indicate regions of significantly lower and higher uptakes in the aged group as compared with young group. Figures represent sections −19, −1, 8, 23, 38, 45 and 53 mm above the AC-PC line.

noted visually in the bilateral basal ganglia regions in the young group.

Figure 2 shows areas with significant differences in tracer distribution in a voxel by voxel analysis.

In the aged group, statistically significant relative decreases in tracer distribution were found in the left amygdala & parahippocampal gyrus, the left superior temporal gyrus, the left Heschel gyrus, the right superior frontal gyrus, the right anterior cingulate, and bilaterally in the cingulate gyri, the insular cortices and the operculum regions when compared with young normals. Relative increases were found in the left precentral gyrus, bilaterally in the occipital lobes and the superior parietal lobules, in the corona radiata and in the white matter of the

Table 2 Regions showing distribution changes between two age group

	volume (mm^3)	center of gravity			aged	young
		x	y	z	(counts/voxel)	
lt temporal white matter	1038	39.9	−68.7	−6.0	118.0 ± 6.0	102.6 ± 10.5
rt temporal white matter	2637	−41.0	−40.3	−15.3	112.0 ± 4.7	99.7 ± 3.7
lt temporal white matter	2873	39.5	−34.6	−11.5	109.2 ± 3.3	97.7 ± 6.1
lt postcentral gyrus†	3159	3.8	−41.9	64.1	101.6 ± 8.2	86.6 ± 9.1
lt precuneus	4423	6.1	−67.6	51.8	105.4 ± 7.9	87.8 ± 11.3
lt corona radiata	6941	26.3	4.1	25.2	98.2 ± 5.9	87.3 ± 5.8
lt medial occipitotemporal gyrus	7023	11.7	−94.3	14.2	99.4 ± 8.4	78.6 ± 10.3
rt corona radiata	9053	−27.4	−6.1	19.9	103.9 ± 3.1	93.2 ± 4.0
lt parahippocampal gyrus	1059	15.3	−52.3	1.6	115.9 ± 12.3	124.0 ± 8.5
lt superior temporal gyrus	1073	58.6	−30.7	17.1	123.0 ± 10.5	134.0 ± 6.7
vermis	1089	1.0	−62.4	−19.6	130.2 ± 7.9	140.1 ± 6.5
rt inferior occipital gyrus	1101	−40.5	−71.9	−21.1	100.7 ± 13.0	114.2 ± 10.3
rt middle temporal gyrus	4984	−59.6	−39.9	−3.6	101.8 ± 9.6	116.7 ± 8.5
rt operculum	6597	−42.1	21.2	2.5	108.0 ± 10.6	126.6 ± 8.8
lt cingulate gyrus†	8003	0.8	−12.4	35.6	102.6 ± 10.1	112.3 ± 8.5

The mean and SD SPECT counts for each group, the volumes and Talairach coordinates of selected areas through voxel-by-voxel analysis are shown above. The regions with dagger extend bilateral structures.

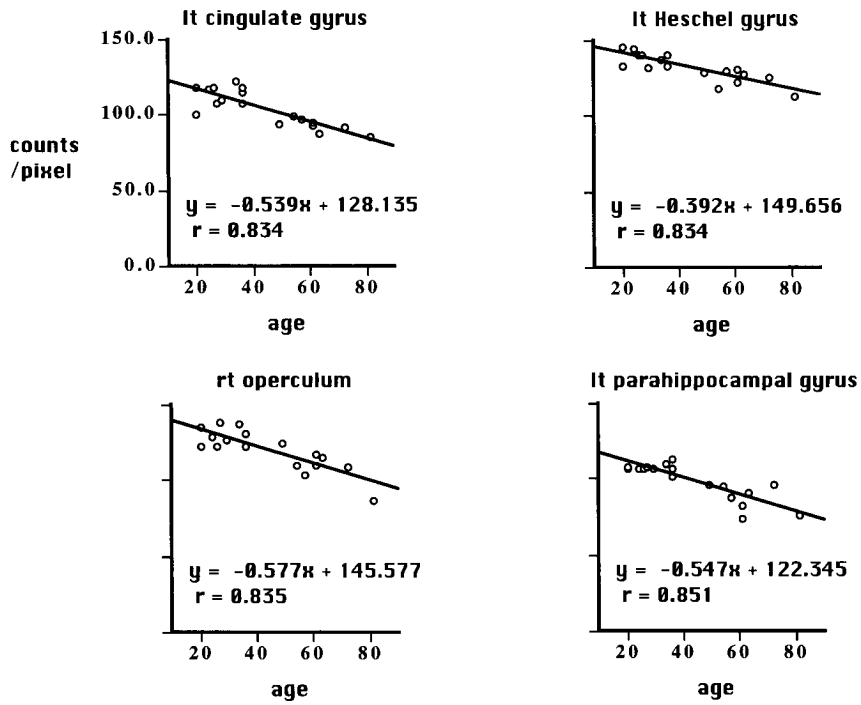

Fig. 3 Examples of age-related changes in tracer distribution. The mean values of normalized SPECT counts within each specific ROI are plotted against the age of the subject. Strong correlations between SPECT counts and age are shown. The results indicate there may be age-related change in the distribution pattern of HMPAO in these specific regions. lt and rt indicate left and right, respectively.

temporal gyri.

Of these areas, we defined ROIs among the original descriptive three-dimension t-value "contour map" images, paying regard to brain anatomical structures (Table 2). Each region had at least a 1,000 mm^3 volume within the specific structure.

Scatter-diagrams of SPECT values against age for the ROIs were made and examined with respect to age-related changes. The left amygdala and the parahippocampal gyrus, the bilateral insular cortices and the operculum regions and the bilateral cingulate gyri demonstrated a tendency to decrease ($r > 0.7$). Conversely, in the left superior parietal lobule and the left corona radiata, the bilateral temporal white matter showed a tendency to

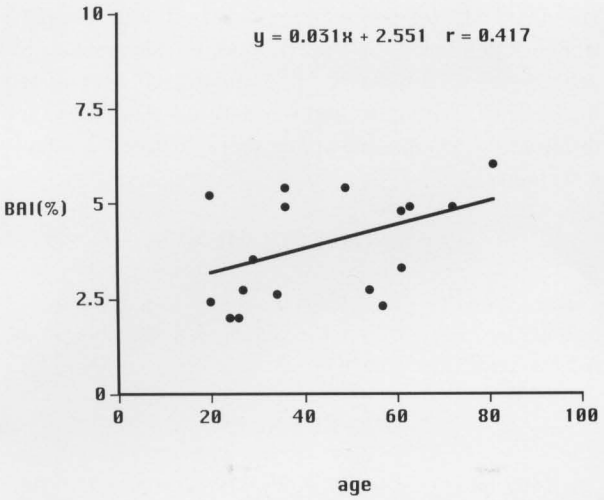

Fig. 4 Brain atrophy indices (BAI) for the subjects. BAI showed a tendency for increase, but this was not statistically significant.

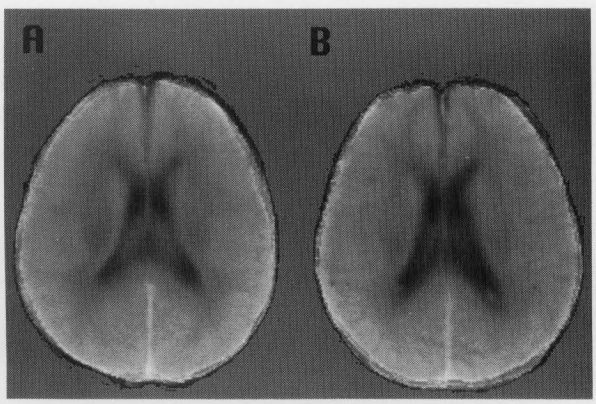

Fig. 5 Mean CT images for each age group. Anatomically standardized CT images for the 10 young subjects (left: A) and the 8 aged subjects (right: B) are presented. Sections are 20 mm above the AC-PC line. There are no significant morphological differences between two groups.

increase ($r > 0.7$). The r values greater than 0.7 correspond to a significance level of $p < 0.01$. Figure 3 exemplifies some significant relationships with r values greater than 0.8.

BAIs for each subject are shown in Table 1, a tendency to increase with age being observed, but this was not significant ($r = 0.42$) in the present study (Figure 4). In addition, Student's t-test showed no statistically significant difference between two groups ($p = 0.16$).

Anatomically standardized CT images (Figure 5) showed no prominent morphological differences between the two groups.

DISCUSSION

Our results show that decreases in relative tracer distribution with age occur in the limbic system, the insular cortices and opercula region and the left temporal cortex. Increases in relative tracer distribution were recognized in the bilateral temporal white matter, the corona radiata and the occipital & parietal regions.

Changes in global cerebral perfusion

The change in whole brain perfusion may affect the distribution pattern of regional perfusion since our method adopts a normalization procedure by means of whole brain perfusion, so that whole brain perfusion as a premise of discussion should be evaluated.

CBF studies with PET have not yet shown consistent results with regard to age-related changes in global CBF. Most authors, however, suggested a global decline in CBF with age, the forerunner being Kety.[11] On the other hand, some concluded,[12,13] that global CBF was subject to personal variation and not age-dependent.

On the "decline" side, the consensus is that decrease in cerebral perfusion in PET studies is more prominent in the gray than in the white matter.[14–16] This implies that the contrast between white and gray matter on the PET image decreases with age and the white matter is relatively enhanced. Meyer et al. showed that cortical gray matter tissue density declines after age 60 and that cortical "polio-araiosis" is coupled with regional hypo-perfusion but not cortical atrophy.[17] Significant negative correlations with age were also reported for the cerebral cortices[14] and especially the frontal cortex.[18,19]

What is evident is that none has reported an increase in whole brain perfusion with aging so far. We can therefore naturally deduce that a pattern of "relative" decrease in tracer distribution with age should be at least a reflection of a decrease in regional blood flow.

Regional changes

With regard to more local brain areas, changes in the tracer distribution pattern with age have yet to be established. In many PET studies focused on regional CBF changes, significant age-related decreases were reported[13–15] with which our results are generally consistent, but Yamaguchi et al. could not detect any significant age-related changes in rCBF.[12] As our aged subjects did not exhibit definite atrophic change with age, it is reasonable to conclude that a change in CBF for the most part brought about the change in SPECT images over possible effect of brain atrophy.

In PET studies, Pantano et al.[16] found the age-related decline in gray matter rCBF preferentially affected the frontal and temporo-sylvian cortices, as well as the parieto-occipital regions. On the other hand, white matter was found to be spared by the aging process. Leenders et al. obtained similar results[15] and also noted that the cerebellar values did not show any age-related change. Pantano et al. pointed to neuronal loss in the prefrontal, precentral and temporal cortices with less involvement of glial cells in the aging process. They also reported a decreased

frontal/sensory-motor cortex ratio. Martin et al. did not specify any significant relationship between global CBF and aging, but described significant negative rCBF correlations with age for the cingulate, parahippocampal, superior temporal, medial frontal, and posterior parietal cortices bilaterally, as well as the left insular and left posterior prefrontal cortices.[14] They also suggested a greater flow decrease in the left hemisphere.

Catafau et al.'s ^{99m}Tc-HMPAO SPECT study of aging[20] in a larger subject population by means of ROI analysis showed rCBF decreases in the left frontal lobe and the posterior region of the left temporal lobe. They further showed "paradoxical" increases in the occipital region. They refer to the decreases as mostly due to brain atrophy. According to them, the increases were not statistically significant when the cerebellum was used as a reference. Provided that cerebellar blood flow is maintained during aging, the "paradoxical" increases would be elucidated as a consequence of CBF decreases in the frontal part of the brain with age. The interpretation is compatible with their results and ours.

With reference to FDG PET studies,[21] intersubject variation seems to promise less consolidated results than with PET perfusion, but a tendency to a decrease in frontal metabolism with age has generally been concluded,[22,23] and this would support our view stated above.

Methodological considerations

As to the accuracy of anatomical standardization, we earlier obtained a standard deviation of approximately 3 mm,[24] which is less than the spatial resolution of the SPECT device. The precision of the reformation process has an SD of 2–3 mm for localization of the brain surfaces and 3–5 mm for the major sulci on the brain surface. If enlargement of the sulci and ventricles accompanies brain atrophy, procedural failure of standardization can take place. But in this study no definite atrophic change was suggested in CT images, as already mentioned. Therefore, when considering the resolution of SPECT images, one can say that mean ROI values represent the mean RI uptake for these specific regions.

In this study, gender segregation was not considered. The structural differences between male and female brains have been reported since the measurement of the corpus callosum by DeLacoste-Utamsing.[25] But if the corpus callosum of the female be thicker than that of the male, the morphological difference does not sufficiently correspond with the functional difference. Further, with the standardization procedure, morphological differences are grossly dismissed. There is no definite consensus for gender difference in cerebral perfusion in such a condition. To examine the gender difference is a plan for the future also for us.

In conclusion, age-related changes exist in HM-PAO distribution patterns. We believe that our findings should contribute to more precise application of the diagnostic HM-PAO SPECT procedure. Compared with the traditional dependence on empirical skill, the present approach offers a firm basis. The standardized, normalized mean SPECT images could constitute a database for different age groups and will be useful in group comparison studies.

ACKNOWLEDGMENTS

This work was partly supported by grants from the National Institute for Longevity Science and the Telecommunications Advancement Organization of Japan.

REFERENCES

1. Kung HF, Ohmomo Y, Kung MP. Current and future radiopharmaceuticals for brain imaging with single photon emission computed tomography. *Semin Nucl Med* 20 (4): 290–302, 1990.
2. Neirinckx RD, Burke JF, Harrison RC, Forster AM, Andersen AR, Lassen NA. The retention mechanism of technetium-99m-HM-PAO: intracellular reaction with glutathione. *J Cereb Blood Flow & Metab* 8: S4–12, 1988.
3. Roland PE, Graufelds CJ, Wahlin J. Human brain atlas: For high-resolution functional and anatomical mapping. *Hum Brain Mapp* 1: 173–184, 1994.
4. Ito H, Kawashima R, Awata S, Ono S, Sato K, Goto R, et al. Hypoperfusion in the limbic system and prefrontal cortex in depression: SPECT with anatomic standardization technique. *J Nucl Med* 37: 410–414, 1996.
5. Koyama M, Kawashima R, Ito H, Ono S, Sato K, Goto R, et al. SPECT imaging of normal subjects with technetium-99m-HMPAO and technetium-99m-ECD. *J Nucl Med* 38: 587–592, 1997.
6. Hatta T, Nakatuka Z. Handedness inventory. *Papers on Celebrating 63rd Birthday of Prof. Ohnishi*, pp. 224–245, 1975.
7. Takeda S, Matsuzawa T. Brain atrophy during aging: A quantitative study using computed tomography. *J Am Geriatr Society* 32: 520, 1984.
8. Budinger TF, Gullberg GT, Huesman RH. *Image reconstruction from projections*, Herman GT, ed. New York: Springer-Verlag p. 197, 1979.
9. Chang LT. Attenuation correction and incomplete projection in single photon emission computed tomography. *IEEE Trans Nucl Sci* 26: 2780–2789, 1979.
10. Chang LT. A method for attenuation correction in radionuclide compute tomography. *IEEE Trans Nucl Sci* 25: 638–646, 1978.
11. Kety S. Human cerebral blood flow and oxygen consumption as related to aging. *J Clin Invest* 8: 478–486, 1956.
12. Yamaguchi T, Kanno I, Uemura K, Shishido F, Inugami A, Ogawa T, et al. Reduction in regional cerebral metabolic rate of oxygen during human aging. *Stroke* 17: 1220–1228, 1986.
13. Itoh M, Hatazawa J, Miyazawa H, Matsui H, Meguro K, Yanai K, et al. Stability of cerebral blood flow and oxygen metabolism during normal aging. *Gerontology* 36: 43–48, 1990.
14. Martin AJ, Friston KJ, Colebatch JG, Frackowiak RS.

Decreases in regional cerebral blood flow with normal aging. *J Cereb Blood Flow & Metab* 11: 684–689, 1991.
15. Leenders KL, Perani D, Lammertsma AA, Heather JD, Buckingham P, Healy MJ, et al. Cerebral blood flow, blood volume and oxygen utilization. Normal values and effect of age. *Brain* 113 (Pt 1): 27–47, 1990.
16. Pantano P, Baron JC, Lebrun-Grandie P, Duquesnoy N, Bousser MG, Comar D. Regional cerebral blood flow and oxygen consumption in human aging. *Stroke* 15: 635–641, 1984.
17. Meyer JS, Takashima S, Terayama Y, Obara K, Muramatsu K, Weathers S. CT changes associated with normal aging of the human brain. *J Neurol Sci* 123: 200–208, 1994.
18. Matsuda H, Tsuji S, Shuke N, Sumiya H, Tonami N, Hisada K. Noninvasive measurements of regional cerebral blood flow using technetium-99m hexamethylpropylene amine oxime. *Eur J Nucl Med* 20: 391–401, 1993.
19. Waldemar G, Hasselbalch SG, Andersen AR, Delecluse F, Petersen P, Johnsen A, et al. ^{99m}Tc-d,l-HMPAO and SPECT of the brain in normal aging. *J Cereb Blood Flow & Metab* 11: 508–521, 1991.
20. Catafau AM, Lomena FJ, Pavia J, Parellada E, Bernardo M, Setoain J, et al. Regional cerebral blood flow pattern in normal young and aged volunteers: a ^{99m}Tc-HMPAO SPET study. *Eur J Nucl Med* 23: 1329–1337, 1996.
21. Wang GJ, Volkow ND, Wolf AP, Brodie JD, Hitzemann RJ. Intersubject variability of brain glucose metabolic measurements in young normal males. *J Nucl Med* 35: 1457–1466, 1994.
22. Moeller JR, Ishikawa T, Dhawan V, Spetsieris P, Mandel F, Alexander GE, et al. The metabolic topography of normal aging. *J Cereb Blood Flow & Metab* 16: 385–398, 1996.
23. Loessner A, Alavi A, Lewandrowski KU, Mozley D, Souder E, Gur RE. Regional cerebral function determined by FDG-PET in healthy volunteers: normal patterns and changes with age. *J Nucl Med* 36: 1141–1149, 1995.
24. Koyama M, Kawashima R, Ito H, Ono S, Sato K, Goto R, et al. Normal cerebral perfusion of ^{99m}Tc-HMPAO brain SPECT—evaluation by an anatomical standardization technique. *KAKU IGAKU (Jpn J Nucl Med)* 32: 969–977, 1995.
25. De Lacoste-Utamsing C, Holloway RL. Sexual dimorophism in the human corpus callosum. *Science* 216: 1431–1432, 1982.